

Classical Instability Effects on Photon Excitations and Entanglement

Radouan Hab-arrih^a, Ahmed Jellal^{*a,b} and Abdeldjalil Merdaci^c

^a*Laboratory of Theoretical Physics, Faculty of Sciences, Chouaib Doukkali University,
PO Box 20, 24000 El Jadida, Morocco*

^b*Canadian Quantum Research Center, 204-3002 32 Ave Vernon,
BC V1T 2L7, Canada*

^c*Faculté des Sciences, Université 20 Août 1955 Skikda,
BP 26, Route El-Hadaiek 21000, Algeria*

Abstract

The Schrödinger dynamics of photon excitation numbers together with entanglement in two non-resonant time-dependent coupled oscillators is investigated. By considering π -periodically pumped parameters and using suitable transformations, we obtain the coupled Meissner oscillators. Consequently, our analytical study shows two interesting results, which can be summarized as follows. (i): Classical instability of classical analog of quantum oscillators and photon excitation averages $\langle N_j \rangle$ are strongly correlated. (ii): Photon excitation's and entanglement are connected to each other. These results can be used to shed light on the link between quantum systems and their classical counterparts. Also it allow to control entanglement by engineering only classical systems where the experiments are less expensive.

PACS numbers: 03.65.Fd, 03.65.Ge, 03.65.Ud, 03.67.Hk

Keywords: Classical instability maps, time-dependent coupled oscillators, photon excitation's, entanglement, Ermakov equation, Meissner equation.

*a.jellal@ucd.ac.ma

1 Introduction

Since the emergence of quantum theory (QT) in the beginning of 20th century, entanglement was used to refute the basic QT's principles. In the early stages, Einstein, Podolsky and Rosen (EPR) [1] (known as EPR paper), have attacked violently QT by remarking that wave functions can be entangled, which entails in their point of view the existence of hidden variables. In other part, entanglement was considered as a necessary complement of QT because without it, it is impossible to interpret and confirm the previsions of QT [2]. Actually, entanglement plays an important role in quantum information processing protocols and it is considered a necessary resource to go beyond the classical communications and technologies.

In the last years, controlling entanglement in time-dependent coupled harmonic oscillators was extensively studied, especially when oscillator systems in contact with environment. For instance, It was shown that the possibility to generate entanglement by phasing control in two [3] and three [4] isotropic harmonic oscillator's sinusoidally coupled to each other by $c(t) = c_0 \cos(\omega t)$ and weakly coupled to an harmonic bath. It was found that the survival of entanglement for a large simulation time is due to instability of decoupled (from the bath) normal oscillator [5]. More recently, it was shown that the vacuum $|G\rangle$ of two time-independent resonant oscillators contains virtual excitation's [6], i.e. $\langle G|a^+a|G\rangle = \langle G|b^+b|G\rangle \neq 0$, in the range of strong coupling, which a consequence of the counter-rotating terms appearing in the Hamiltonian. As a result, the presence of these excitation's maintains entanglement between oscillators.

Motivated by the above studies, we address to the question: how classical instabilities affect photon excitation's and consequently entanglement in the vacuum of two time-dependent non-resonant coupled harmonic oscillators. Our response will be given in the framework of an assumption based on the fact that our harmonic oscillators are connected by a periodically quenched coupling parameter $J(t) = J_0\Theta(t)$ and having perturbed frequencies $\omega_{1,2}^2(t) = \omega_0^2 \pm \epsilon\Theta(t)$, with Θ is a π -periodic function $\Theta(t) = \Theta(t + \pi)$ and ϵ is the quench amplitude. As a result, we end up with an integrable model called two coupled Meissner oscillators [7]. This kind of oscillators can be seen, for instance, as LC_0 oscillator with the parametric frequency $\omega_0^2 = (LC_0)^{-1}$ where the capacitance C_0 is pumped by a voltage $V(t)$ such that $C_0 \rightarrow C(t) = C_0 + C_p\Theta(t)$ ($C_p < C_0$) [8], or as a charged pendulum in alternating, piecewise constant, homogeneous electric field [9]. The resolution of the Schrödinger dynamics allows us to find Ermakov equations [10] and utilization of suitable transformations leads to get two Meissner differential equations corresponding to classical counterparts of the decoupled Hamiltonian. Then, we study the instabilities of derived differential equations and show instability/stability diagrams. With these, we be able to investigate the link between two strongly different features: the photon excitation's and classical instabilities. Additionally, by computing logarithmic negativity we establish a bijection between entanglement and photon excitation's.

The layout of our paper is given as follows. In Sec. 2, we present our model and show how to exactly decouple the Hamiltonian system by using suitable transformations. The instabilities of emerged equations of both Ermakov and Meissner will be discussed in Sec. 3. We compute entanglement by using logarithmic negativity and quantifying excitation in both oscillators by averaging the number operators over the vacuum in Sec. 4. We show our numerical results and present different discussions in Sec. 5. Finally, we give an exhaustive conclusion to our work.

2 Model and Schrödinger dynamics

2.1 Model and integrability

The main concern in the present work is to answer the question asked in our introduction. Mainly about how the classical instabilities affect photon excitation's and therefore entanglement in the vacuum of two time-dependent non-resonant coupled harmonic oscillators (Figure 1) described by the Hamiltonian

$$H(\hat{x}_1, \hat{x}_2) = \frac{\hat{p}_1^2}{2} + \frac{\hat{p}_2^2}{2} + \frac{1}{2}\omega_1^2(t)\hat{x}_1^2 + \frac{1}{2}\omega_2^2(t)\hat{x}_2^2 - J(t)\hat{x}_1\hat{x}_2 \quad (1)$$

where $\omega_j(t)$ are the frequencies and $J(t)$ is a coupling parameter, with $j = 1, 2$. For simplicity, we assume that the masses are unit (we set the masses as equal to one, because, as Macedo and Guedes showed [11], a simple transformation may be applied that makes the assumption valid) and $\hbar = 1$.

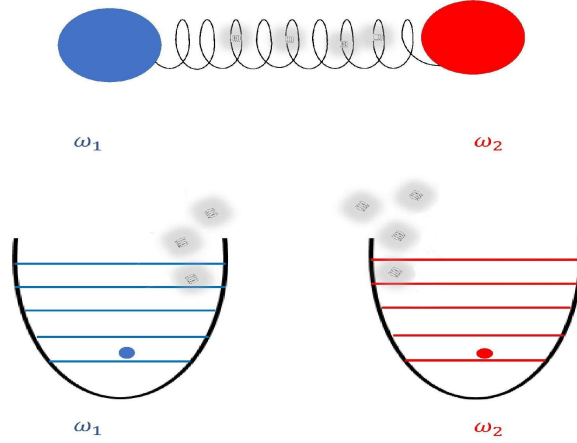


Figure 1 – (color online) The schematic shows two coupled oscillators via a position-position coupling type $x_1 x_2$. The particles still in their vacuum. The dynamics generates virtual excitation's between oscillators that affect quantum quantities.

Since the Hamiltonian (1) is involving an interacting term, then a straightforward diagonalization is not an easy task. To overcome such situation, we introduce the time-dependent rotation with an angle $\alpha(t)$

$$\mathcal{R}_\alpha(t) = \exp[-i\alpha(t)\hat{L}_z], \quad \alpha(t) = \frac{1}{2} \arctan\left(\frac{2J(t)}{\omega_1^2(t) - \omega_2^2(t)}\right) \quad (2)$$

in terms of the angular momentum $\hat{L}_z = \hat{x}_1\hat{p}_2 - \hat{x}_2\hat{p}_1$. Consequently, the transformed Hamiltonian is given by

$$\tilde{H}(\hat{x}_1, \hat{x}_2) = \mathcal{R}_\alpha(t)H(\hat{x}_1, \hat{x}_2)\mathcal{R}_\alpha^{-1}(t) - i\mathcal{R}_\alpha(t)\partial_t\mathcal{R}_\alpha^{-1}(t) \quad (3)$$

and after some algebras, we obtain

$$\tilde{H}(\hat{x}_1, \hat{x}_2) = \frac{\hat{p}_1^2}{2} + \frac{\hat{p}_2^2}{2} + \frac{1}{2}\Omega_1^2(t)\hat{x}_1^2 + \frac{1}{2}\Omega_2^2(t)\hat{x}_2^2 + \dot{\alpha}(t)(\hat{x}_1\hat{p}_2 - \hat{x}_2\hat{p}_1) \quad (4)$$

where we have defined the frequencies Ω_j

$$\Omega_{1,2}^2(t) = \frac{1}{2} \left(\omega_1^2(t) + \omega_2^2(t) \pm \sqrt{[\omega_1^2(t) - \omega_2^2(t)]^2 + 4J^2(t)} \right). \quad (5)$$

For the boundness of Hamiltonian, the physical parameters point $\mathcal{P}(\omega_1, \omega_2, J)$ should belongs to the physical $3D$ -space

$$\mathcal{E}_B = \{\mathcal{P} / \omega_1^2 \omega_2^2 > J^2\} \quad (6)$$

It is clearly seen from (4) that the separation of variables is possible for $\dot{\alpha}(t) = 0$, which is equivalent to have

$$\tan(2\alpha(t)) = \frac{2J(t)}{\omega_1^2(t) - \omega_2^2(t)} = \text{constant} \quad (7)$$

which has been used also in different occasions, one may see for instance [11, 12]. Then the Hamiltonian is decoupled and canonically is equivalent to the following time-dependent harmonic oscillators

$$\tilde{H}(\hat{x}_1, \hat{x}_2) = \frac{\hat{p}_1^2}{2} + \frac{1}{2}\Omega_1^2(t)\hat{x}_1^2 + \frac{\hat{p}_2^2}{2} + \frac{1}{2}\Omega_2^2(t)\hat{x}_2^2 = \tilde{H}_1(\hat{x}_1) + \tilde{H}_2(\hat{x}_2) \quad (8)$$

which can easily be solved to extract the solutions of energy spectrum and then solve different issues related to our system.

2.2 Time-dependent Schrödinger equation

The commutativity $[\tilde{H}_1, \tilde{H}_2] = 0$ implies that the solutions of time-dependent Schrödinger equation have the forms

$$\tilde{\Psi}(x_1, x_2; t) = \tilde{\phi}_1(x_1; t) \otimes \tilde{\phi}_2(x_2; t) \quad (9)$$

where each $\tilde{\phi}(x_j; t)$ satisfies

$$\left(-\frac{1}{2}\partial_{x_j}^2 + \frac{1}{2}\Omega_j^2(t)\hat{x}_j^2\right)\tilde{\phi}_j(x_j; t) = -i\partial_t\tilde{\phi}_j(x_j; t), \quad j = 1, 2. \quad (10)$$

This was earlier studied in [13] and then the general solution of the Schrödinger equation is a superposition of orthonormal expanding modes $\tilde{\psi}(x_j; t) = \sum_{n=0} \mathfrak{p}_{n_j}(t)\tilde{\phi}_j(x_j, t)$, with $\sum_{n_j=0} |\mathfrak{p}_{n_j}(t)|^2 = 1$. It follows that for a single mode and $\Omega_j^2(0) > 0$, we have

$$\tilde{\phi}_j(x_j; t) = \exp\left[-i\left(n_j + \frac{1}{2}\right)\int_0^t \varpi_j(\tau)d\tau\right] \chi_{n_j}(x_j; t) \quad (11)$$

and the orthogonal Hermite polynomials are

$$\chi_{n_j}(x_j; t) = \frac{1}{\sqrt{2^{n_j} n_j!}} \left(\frac{\varpi_j(t)}{\pi}\right)^{\frac{1}{4}} \exp\left[-\frac{1}{2}\varpi_j(t)x_j^2\right] \mathcal{H}_{n_j}\left(\sqrt{\varpi_j(t)}x_j\right) \quad (12)$$

where we have defined the scaling frequencies as $\varpi_j(t) = \frac{\Omega_j(0)}{h_j^2(t)}$. The functions $h_j(t)$ are solutions of Ermakov equations (dots stand for time derivatives hereafter)

$$\ddot{h}_j + \Omega_j^2(t)h_j = \frac{\Omega_j^2(0)}{h_j^3} \quad (13)$$

and satisfy the initial conditions $h_j(0) = 1, \dot{h}_j(0) = 0$. It is worthy to note that the energy spectrum is time-independent

$$E_{n_j} = \left(n_j + \frac{1}{2}\right)\Omega_j(0) \quad (14)$$

whereas the average of energy is time-dependent because we have

$$\langle \tilde{H}(x_j; t) \rangle_{n_j} = \frac{2n_j + 1}{4\Omega_j(0)} \left(\dot{h}_j^2 + \Omega_j^2(t) h_j^2 + \frac{\Omega_j^2(0)}{h_j^2} \right). \quad (15)$$

Consequently the eigenfunctions of decoupled Hamiltonian are given by

$$\begin{aligned} \tilde{\Psi}_{n_1, n_2}(x_1, x_2; t) &= \frac{1}{\sqrt{2^{n_1+n_2} n_1! n_2!}} \left(\frac{\varpi_1(t) \varpi_2(t)}{\pi^2} \right)^{\frac{1}{4}} \mathcal{H}_{n_1} \left(\sqrt{\varpi_1(t)} x_1 \right) \mathcal{H}_{n_2} \left(\sqrt{\varpi_2(t)} x_2 \right) \\ &\times \exp \left[-i \left(n_1 + \frac{1}{2} \right) \int_0^t \varpi_1(\tau) d\tau - i \left(n_2 + \frac{1}{2} \right) \int_0^t \varpi_2(\tau) d\tau \right] \\ &\times \exp \left[\frac{i}{2} \left(\frac{\dot{h}_1}{h_1} - i\varpi_1(t) \right) x_1^2 + \frac{i}{2} \left(\frac{\dot{h}_2}{h_2} - i\varpi_2(t) \right) x_2^2 \right]. \end{aligned} \quad (16)$$

Now by performing the reciprocal rotation $\mathcal{R}_{-\alpha}(t)$, we end up with the single mode solution of the Hamiltonian (1), which is

$$\begin{aligned} \Psi_{n_1, n_2}(x_1, x_2; t) &= \mathcal{R}_{-\alpha}(t) \tilde{\Psi}_{n_1, n_2}(x_1, x_2; t) \\ &= \tilde{\Psi}_{n_1, n_2}(x_1 \cos \alpha - x_2 \sin \alpha, x_1 \sin \alpha + x_2 \cos \alpha; t). \end{aligned} \quad (17)$$

In the forthcoming analysis, we only consider the following vacuum solution

$$\begin{aligned} \Psi_{0,0}(x_1, x_2; t) &= \left(\frac{\varpi_1(t) \varpi_2(t)}{\pi^2} \right)^{\frac{1}{4}} \exp \left[-\frac{i}{2} \int_0^t \varpi_1(\tau) d\tau - \frac{i}{2} \int_0^t \varpi_2(\tau) d\tau \right] \\ &\times \exp \left[-\frac{1}{2} \mathcal{A}_1(t) x_1^2 - \frac{1}{2} \mathcal{A}_2(t) x_2^2 + \mathcal{A}_{12}(t) x_1 x_2 \right] \end{aligned} \quad (18)$$

where the involved time-dependent parameters read as

$$\mathcal{A}_1(t) = \varpi_1(t) \cos^2 \alpha + \varpi_2(t) \sin^2 \alpha - i \left(\frac{\dot{h}_1}{h_1} \cos^2 \alpha + \frac{\dot{h}_2}{h_2} \sin^2 \alpha \right) \quad (19)$$

$$\mathcal{A}_2(t) = \varpi_1(t) \sin^2 \alpha + \varpi_2(t) \cos^2 \alpha - i \left(\frac{\dot{h}_1}{h_1} \sin^2 \alpha + \frac{\dot{h}_2}{h_2} \cos^2 \alpha \right) \quad (20)$$

$$\mathcal{A}_{12}(t) = \sin \alpha \cos \alpha \left[\varpi_1(t) - \varpi_2(t) + i \left(\frac{\dot{h}_2}{h_2} - \frac{\dot{h}_1}{h_1} \right) \right]. \quad (21)$$

These results will be used to compute the number of occupation and discuss entanglement through the logarithmic negativity.

3 Classical stability and differential equations

As we have seen above the vacuum state (18) is strongly depending on the functions h_1 and h_2 solutions of Ermakov equations (13). Then it is of interest to discuss the classical stability and instability related to Ermakov equation by deriving the conditions of classical stabilities. In the beginning, let us perform the following transformation on h_1 and h_2 [14]

$$\mathbb{X}(t) = h_1(t) e^{i \int_0^t \varpi_1(s) ds} \quad (22)$$

$$\mathbb{Y}(t) = h_2(t) e^{i \int_0^t \varpi_2(s) ds} \quad (23)$$

to obtain the Hill system

$$\ddot{\mathbb{X}} + \Omega_1^2(t)\mathbb{X} = 0 \quad (24)$$

$$\ddot{\mathbb{Y}} + \Omega_2^2(t)\mathbb{Y} = 0 \quad (25)$$

describing the two decoupled classical time-dependent harmonic oscillators of frequencies $\Omega_1(t)$ and $\Omega_2(t)$. Now it is clear that the stability of Hill system solutions leads to find that of Ermakov one and therefore $h_j(t)$ can be expressed as [10]

$$h_1^2(t) = x_1^2(t) + \Omega_1^2(0)W^{-2}[x_1, x_2]x_2^2(t) \quad (26)$$

$$h_2^2(t) = y_1^2(t) + \Omega_2^2(0)W^{-2}[y_1, y_2]y_2^2(t). \quad (27)$$

such that x_j and y_j are independent solutions of (24) and (25), respectively, satisfying the initial conditions $x_1(0) = y_1(0) = 1$ and $x_2(0) = y_2(0) = 0$. Both Wronskian $W[x_1, x_2] = x_1\dot{x}_2 - x_2\dot{x}_1$ and $W[y_1, y_2] = y_1\dot{y}_2 - y_2\dot{y}_1$ are constant.

To proceed further, we require some conditions on frequencies and coupling parameter [8,9]. Indeed, let us modulate them as

$$\omega_{1,2}^2(t) = \omega_0^2 \pm \epsilon\Theta(t), \quad J(t) = J_0\Theta(t) \quad (28)$$

where ω_0 , J_0 , and ϵ are the parametric frequency, coupling amplitude and quench amplitude, respectively. The involved π -periodic quencher $\Theta(t)$ is defined by

$$\Theta(t) = \begin{cases} +1 & 0 \leq t < \frac{\pi}{2} \\ -1 & \frac{\pi}{2} \leq t < \pi \end{cases} \quad (29)$$

and then the frequencies (5) reduce to the following

$$\Omega_{1,2}^2(t) = \omega_0^2 \pm \Theta(t)\sqrt{\epsilon^2 + J_0^2}. \quad (30)$$

It is worthy to note that with the modulation (28), the Hill system (24-25) reduces to the Meissner equations [9]. Now, we discuss the boundness of Hamiltonian because the solutions presented in (18) are only valid for $\Omega_j(0) > 0$, with $j = 1, 2$ [15]. As a result of (28) the boundness condition (6) becomes $\omega_0^4 - \epsilon^2 > J_0^2$, which is equivalent to an open disc of center $(J_0^2 = 0, \epsilon^2 = 0)$ and radius $R = \omega_0^2$. In Figure 2, we give the physical maps for boundness of Hamiltonian in two different configurations (ϵ, J_0) and (ω_0^2, J_0) . The maps show that the unbound regions are very large than bound ones, which limits our choices. Note that, the edges of boundness present great importance for example in generating important entanglement and leading to inverse engineering of time-dependent coupled harmonic oscillators [16].

To study the classical instability of (24-25), we will use the discrete transition matrix formalism or Floquet exponents technique [8]. Then, after some algebra we show that of the stability condition of two oscillators can be written as

$$\mathcal{S} := \max[1 - \Lambda(\Omega_1, \Omega_2), 0] > 0 \quad (31)$$

where Λ is a dimensionless parameter

$$\Lambda(\Omega_1, \Omega_2) = \left| \cos\left(\frac{\Omega_1\pi}{2}\right) \cos\left(\frac{\Omega_2\pi}{2}\right) - \frac{1}{2} \left(\frac{\Omega_1}{\Omega_2} + \frac{\Omega_2}{\Omega_1}\right) \sin\left(\frac{\Omega_1\pi}{2}\right) \sin\left(\frac{\Omega_2\pi}{2}\right) \right|. \quad (32)$$

In Figure 3, we numerically show the stability diagram in the physical configuration (ϵ, ω_0^2) . It is clearly seen that the stability diagram is very sensitive to the physical parameters because a small change produces important configuration variation. We notice that the instability region increases as long as the coupling parameter increases. This in fact tells us that why one has to investigate the effect of instabilities on the quantum features.

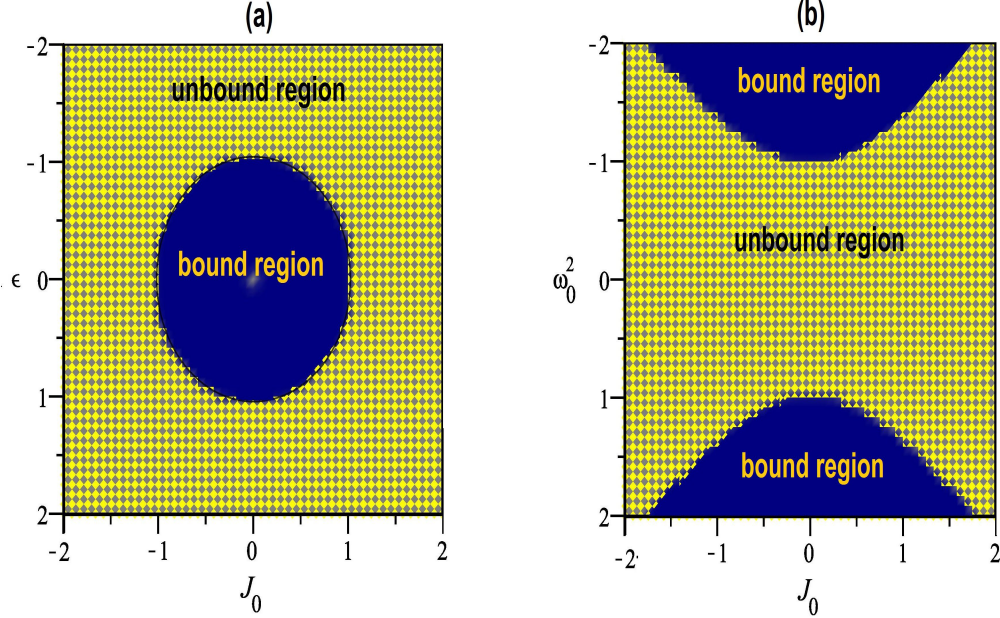


Figure 2 – (color online) The boundness maps in two space configurations. (a): Configuration (ϵ, J_0) for $\omega_0^2 = 1$, as predicted the physical points that bound the Hamiltonian (1) form an open disc of radius $R = \omega_0^2 = 1$. (b): Configuration (ω_0^2, J_0) for $\epsilon = 1$.

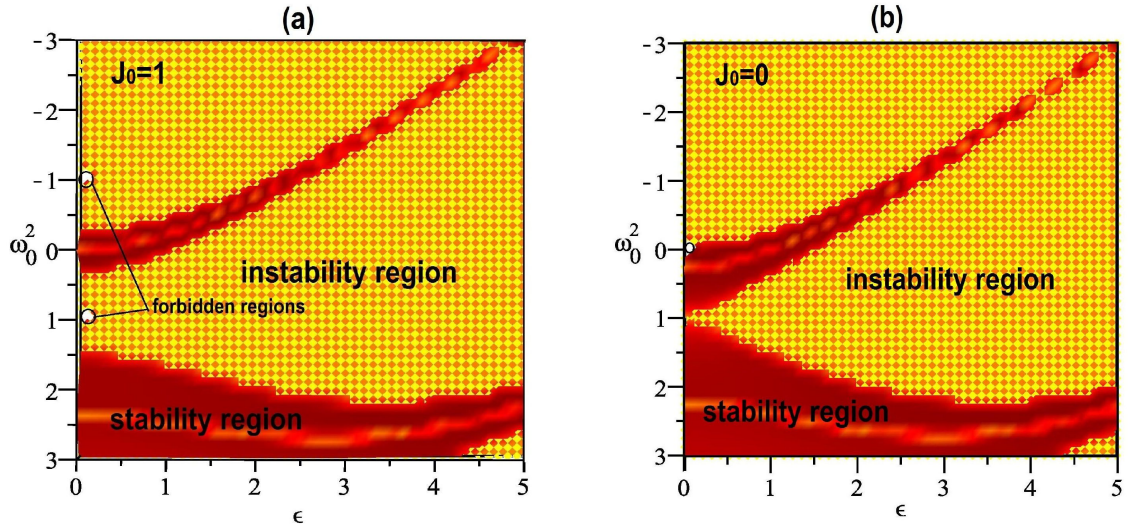


Figure 3 – (color online) The stability diagram of Meissner system (24-25) with modulation (28) in the space configuration (ϵ, ω_0) for two cases (a): $J_0 = 0$ and (b): $J_0 = 1$. The yellow area stands for instability region ($S = 0$), red area for stable region ($S > 0$), white dots for forbidden parameters ($\Omega_2(0) = 0$).

4 Entanglement and photon excitation's

4.1 Entanglement and dynamics effects

According to Peres-Horodecki criterion, [17, 18], the necessary and sufficient condition for the separability of two Gaussian mode states is the positivity of the partially transposed state. Since the vacuum state (18) is pure and symmetric, then separability can be realized by switching (21) to zero, namely having the condition

$$\mathcal{A}_{12}(t) = 0 \quad (33)$$

which is necessary and sufficient for separability and obviously it is achieved in two subordinate cases, (i): for $J_0 = 0$ the dynamics can not generate entanglement and the oscillators still separable during the dynamics, (ii): for the Wronskian $W[h_1(t), h_2(t)] = 0$ and $\varpi_1(t) = \varpi_2(t)$ where the geometrical meaning of W is subtraction of the rectangular phase space areas $S_1 = h_1 \dot{h}_2$ and $S_2 = h_2 \dot{h}_1$ [16]. The last case indicates that the dynamics can extinct entanglement and then to avoid its extinction, the engineering of initial and final normal frequencies $\Omega_j(t_f)$, $\Omega_j(0)$ ($j = 1, 2$) deserves a suitable tuning.

Regarding our case, the vacuum state is completely described by the marginal purities μ_j , ($j = 1, 2$) given by

$$\mu_1(t) = \mu_2(t) := \mu(t) = \left(\frac{\varpi_1(t)\varpi_2(t)}{\varpi_1(t)\varpi_2(t) + |\mathcal{A}_{12}(t)|^2} \right)^{\frac{1}{2}}. \quad (34)$$

Since our state is pure and Gaussian, then all quantum correlation can be derived from the second moment of it, that is the covariance matrix (CM) $\mathcal{V}(t)$. Such CM can be transformed via a local symplectic transformation $S = S_1 \oplus S_2$ to a particular form called standard form $\mathcal{V}_{sf}(t)$ [17]

$$\mathcal{V}_{sf}(t) = \begin{pmatrix} \mu^{-1} & 0 & \sqrt{\mu^{-2} - 1} & 0 \\ 0 & \mu^{-1} & 0 & -\sqrt{\mu^{-2} - 1} \\ \sqrt{\mu^{-2} - 1} & 0 & \mu^{-1} & 0 \\ 0 & -\sqrt{\mu^{-2} - 1} & 0 & \mu^{-1} \end{pmatrix} = \begin{pmatrix} A & C \\ C & A \end{pmatrix}. \quad (35)$$

By performing the partial transposition (PT) prescription, $\det(A) \rightarrow \det(A)$ and $\det(C) \rightarrow -\det(C)$, then the minimal symplectic eigenvalue of the PT covariance matrix $\tilde{\mathcal{V}}$ is

$$\lambda_{min}^2(t) = \frac{1}{2} \left(\Delta(\tilde{\mathcal{V}}) - \sqrt{\Delta^2(\tilde{\mathcal{V}}) - 4} \right) \quad (36)$$

and after evaluation, we find

$$\lambda_{min}^2(t) = \left(1 + \frac{|\mathcal{A}_{12}(t)|^2}{\varpi_1(t)\varpi_2(t)} \right) \left(1 - \sqrt{1 - \mu^2(t)} \right) - 1 \quad (37)$$

where the symplectic invariant is $\Delta(\tilde{\mathcal{V}}) = 2(\det(A) - \det(C))$. Consequently, the logarithmic negativity is given by

$$E_{\mathcal{N}}(t) = \max(0, -\log[\lambda_{min}(t)]) \quad (38)$$

which is monotonically increasing with $|\mathcal{A}_{12}|^2$. From its expression (21) it appears that the main contributions of the time-dependent Hamiltonian is the emergence of an imaginary part, that is $\left(\frac{h_2}{h_2} - \frac{h_1}{h_1} \right)$ and initial normal mode scaling, i.e. $\Omega_j(0) \rightarrow \varpi_j(t) = \frac{\Omega_j(0)}{h_j^2(t)}$.

4.2 Photon excitation's

Using of the phase space prescription [19], we will analyze photon excitation's by computing the average of photon numbers $\langle a_j^\dagger a_j \rangle$ in the vacuum state. The case of two resonant time-independent coupled oscillators was analyzed in [6] where the creation $a_{j,0}^\dagger$ and annihilation $a_{j,0}$ operators are simply mapped as

$$(a_{j,0}^\dagger)^+ = a_{j,0} = \sqrt{\frac{\omega_j}{2}} x_j + \frac{i}{\sqrt{2\omega_j}} p_j. \quad (39)$$

However for time-dependent Hamiltonian, the situation is not obvious because the realization can be done as follows [20, 21]

$$(a_j^\dagger)^+ = a_j = e^{i \int_0^s \eta_j(s) ds} \frac{1}{\sqrt{2\eta_j}} \left[\eta_j \left(1 - i \frac{\dot{\nu}_j}{\nu_j \eta_j} \right) x_j + i p_j \right] \quad (40)$$

where $[a_j, a_j^\dagger] = \mathbb{I}$, $\eta_j(t) = \frac{\omega_j(0)}{\nu_j^2}$ and the functions ν_j satisfy the Ermakov equations

$$\ddot{\nu}_j + \omega_j^2(t) \nu_j = \frac{\omega_j^2(0)}{\nu_j^3}, \quad j = 1, 2. \quad (41)$$

After a straightforward algebra, one can compute the average of photon number operators $N_j = a_j^\dagger a_j$ to end up with

$$\langle N_j \rangle(t) = \frac{1}{2\omega_j(0)} \left(\frac{\omega_j^2(0)}{\nu_j^2} + \dot{\nu}_j^2 \right) \langle \hat{x}_j^2 \rangle_t + \frac{\nu_j^2}{2\omega_j(0)} \langle \hat{p}_j^2 \rangle_t - \frac{\nu_j \dot{\nu}_j}{\omega_j(0)} \langle \hat{x}_j \hat{p}_j \rangle_t - \frac{1}{2} \quad (42)$$

and different averages are explicitly given by

$$\langle \hat{x}_j^2 \rangle_t = \frac{\varpi_j(t) \sin^2 \alpha + \varpi_k(t) \cos^2 \alpha}{2\varpi_j(t) \varpi_k(t)} \quad (43)$$

$$\langle \hat{p}_j^2 \rangle_t = \frac{1}{2} \left[\varpi_j(t) \cos^2 \alpha + \varpi_k(t) \sin^2 \alpha + \frac{1}{\varpi_j(t)} \left(\frac{\dot{h}_j}{h_j} \right)^2 \cos^2 \alpha + \frac{1}{\varpi_k(t)} \left(\frac{\dot{h}_k}{h_k} \right)^2 \sin^2 \alpha \right] \quad (44)$$

$$\langle \hat{x}_j \hat{p}_j \rangle_t = - \frac{\varpi_k(t) \cos^2 \alpha \frac{\dot{h}_j}{h_j} + \varpi_j(t) \sin^2 \alpha \frac{\dot{h}_k}{h_k}}{2\varpi_j(t) \varpi_k(t)} \quad (45)$$

where $k = 1, 2$ and $k \neq j$.

We emphasize that the time-dependent Hamiltonian (1) generates important effects such that the scalings $\eta_j(t) = \frac{\omega_j(0)}{\nu_j^2}$ and $\varpi_j(t) = \frac{\Omega_j(0)}{h_j^2(t)}$, the shiftings in positions (43) and momenta (44), which are due to the dilatation functions $\nu_j(t)$ and $h_j(t)$. In addition, the existence of the term $\langle \hat{x}_j \hat{p}_j \rangle_t$ is purely a consequence of time-dependence, which of course disappears by setting time to zero, namely having constant parameters. Note that, for time-independent Hamiltonian, we have $\nu_j = h_j = 1$ and $\dot{\nu}_j = \dot{h}_j = 0$, then the virtual photon excitation's become

$$\langle N_1 \rangle = \frac{1}{4} \cos^2 \alpha \left(\frac{\Omega_1}{\omega_1} + \frac{\omega_1}{\Omega_1} \right) + \frac{1}{4} \sin^2 \alpha \left(\frac{\Omega_2}{\omega_1} + \frac{\omega_1}{\Omega_2} \right) - \frac{1}{2} \quad (46)$$

$$\langle N_2 \rangle = \frac{1}{4} \sin^2 \alpha \left(\frac{\Omega_2}{\omega_2} + \frac{\omega_2}{\Omega_2} \right) + \frac{1}{4} \cos^2 \alpha \left(\frac{\Omega_1}{\omega_2} + \frac{\omega_2}{\Omega_1} \right) - \frac{1}{2}. \quad (47)$$

In the case of resonant oscillators, i.e. $\omega_1 = \omega_2 = \omega_r$, the rotation angle reduces to $\alpha = \frac{\pi}{4}$. Furthermore, by setting $r_{a,b} = \frac{1}{2} \ln \left(\frac{\Omega_{1,2}}{\omega_r} \right)$, we retain the results derived in [6]

$$\langle N_1 \rangle = \langle N_2 \rangle = \frac{1}{2} (\sinh^2 r_a + \sinh^2 r_b). \quad (48)$$

We mention that the study in [6] was confined on the resonant case because it was not easy to disentangle the rotation operator (2) in the frame of creation a_j^+ and annihilation a_j representation. Now it becomes clear that from our analysis how the phase space picture can be used to overcome such situation. In addition, it is interesting to note that for $\omega_1 \neq \omega_2$ and $J_0 = 0$, the vacuum state (18) contains excitation's, i.e. $\langle N_1 \rangle = \langle N_2 \rangle \neq 0$, even if the oscillators are decoupled, such phenomena does not exist in the frame of resonant oscillators.

5 Results and discussions

Before numerically presenting and discussing the main results derived so far, it is convenient for our task to define dimensionless parameters

$$t \longrightarrow t\Omega_0, \quad \omega_j \longrightarrow \frac{\Omega_j}{\Omega_0}, \quad \epsilon \longrightarrow \frac{\epsilon}{\Omega_0^2}, \quad J_0 \longrightarrow \frac{J_0}{\Omega_0^2} \quad (49)$$

where Ω_0 is an arbitrary frequency. For a numerical study of classical instabilities effects on generation of photon excitation's and hence entanglement between oscillators, we start by giving the dilatation functions h_j and ν_j . Indeed, by using (27) one can solve (13) to obtain the solutions in first period $[0, \pi]$, which are

$$h_1^2(t) = \begin{cases} 1, & 0 \leq t < \frac{\pi}{2} \\ \frac{\Omega_2^2 - \Omega_1^2}{2\Omega_2^2} \cos(2\Omega_2(t - \frac{\pi}{2})) + \frac{\Omega_1^2 + \Omega_2^2}{2\Omega_2^2}, & \frac{\pi}{2} \leq t < \pi \end{cases} \quad (50)$$

$$h_2^2(t) = \begin{cases} 1, & 0 \leq t < \frac{\pi}{2} \\ \frac{\Omega_1^2 - \Omega_2^2}{2\Omega_1^2} \cos(2\Omega_1(t - \frac{\pi}{2})) + \frac{\Omega_1^2 + \Omega_2^2}{2\Omega_1^2}, & \frac{\pi}{2} \leq t < \pi. \end{cases} \quad (51)$$

Note that the solutions of ν_j will be immediately obtained from (50-51) only under the substitution $\sqrt{\epsilon^2 + J_0^2} \longrightarrow \epsilon$. Now, we notice that the freezing dynamics will be occurred in odd half periods while dynamics evolution in even ones, which is due to the periodic quench, and the continuity of solutions h_j and ν_j .

In Figure 4, we remark that vacuum state does not contain virtual excitation's when the classical analog of quantum oscillators are stable and vice verse. Another point that deserves attention is the emergence of excitation's even if the oscillators are decoupled ($J_0 = 0$) and beyond resonance $\omega_1 \neq \omega_2$ ($\epsilon \neq 0$), amazingly the classical oscillators are unstable. Such phenomena is not observed for resonant oscillators [6]. Generally, the virtual photons are originated from counter-rotating (CR) terms ($a_1^+ a_2^+$ and $a_2 a_1$) appearing in the Hamiltonian. However, these terms disappear when the coupling is switched-off and the non-resonance oscillations has no relation with CR. Indeed, the resonance affects the potential energy operator, $V(J_0 = 0) = \frac{1}{2}\omega_1^2(t)\hat{x}_1^2 + \frac{1}{2}\omega_2^2(t)\hat{x}_2^2$, and this does not mix the quadratures \hat{x}_j and \hat{p}_k , then CR terms does not appear. This phenomena can be seen as follows, when the classical oscillators are stable then the virtual excitation's will be suppressed, but for unstable case it will be

created. Note that ϵ and J_0 have the same dimension but different effects on excitation's generation. In order to compare their effects on excitation's amount and hierarchy, we also plot in Figure 4, the dynamics of excitation's $\langle N_1 \rangle$ and $\langle N_2 \rangle$. The numerical results show that the increasing of ϵ increases the amount of excitation's as well as the hierarchy $\langle N_1 \rangle \neq \langle N_2 \rangle$ and changes the topological behavior in the simulate time (linear/sinusoidal). Now, if the values of ϵ and J_0 ($C \leftrightarrow D$) are interchanged, we obtain different aspects, which are due to contributions of ϵ and J_0 in the frequencies ω_j and Ω_j .

In this way, we can affirm that virtual photons are correlated with the instability of classical counterpart's solutions. In our best of knowledge, this phenomena is the first time that it has been studied, and this will lead to control virtual excitation's in quantum systems only by engineering their classical counterparts, where the financial requirements are not enormous. Also it will leads to understand the nature of the connection between quantum systems and theirs classical counterparts.

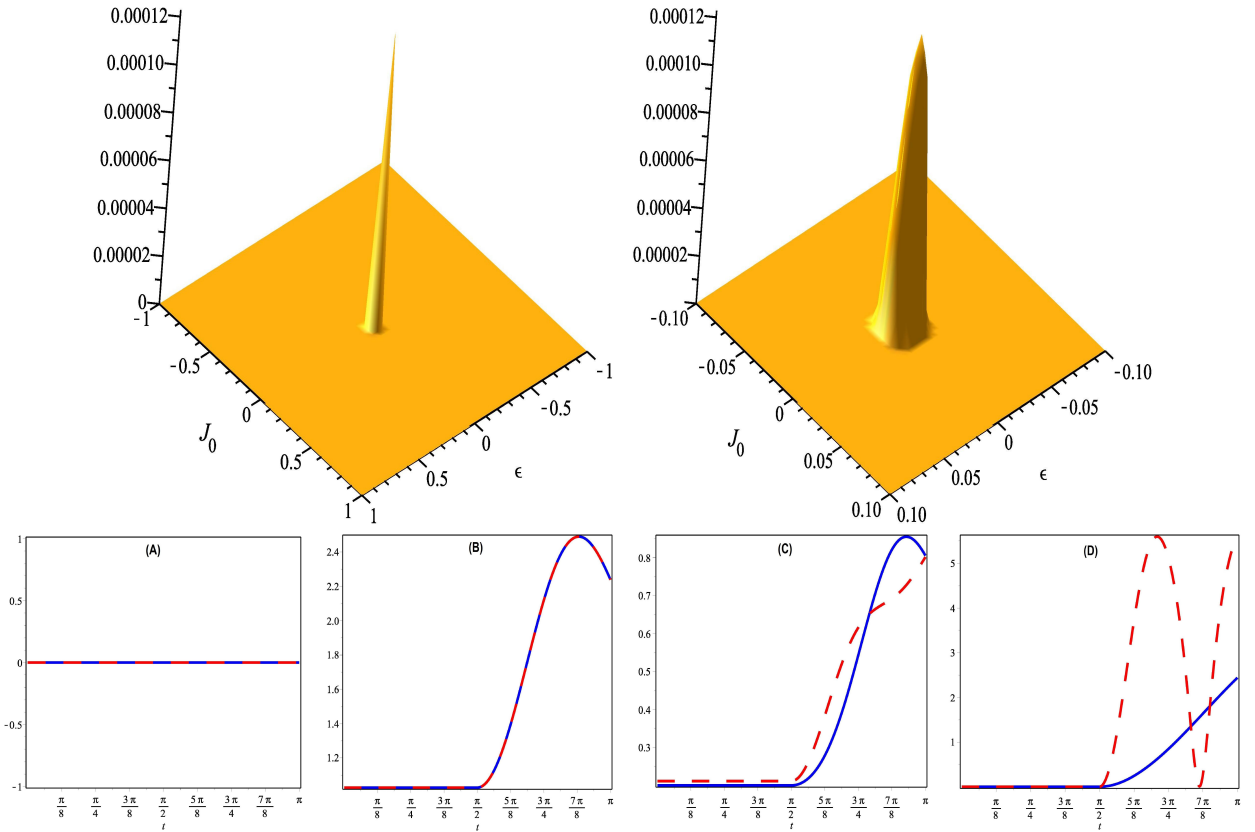


Figure 4 – (color online) The golden surface indicates instability region ($S = 0$) and the stability area ($S > 0$) for the frequency $\omega_0^2 = 1.01$. Panels A, B, C and D present the virtual photon excitation's $\langle N_1 \rangle$ (blue line) $\langle N_2 \rangle$ (red dashed) versus the time t . If we use the notation $M(\epsilon, J_0)$, it turns out that the physical points are $A(0, 0)$, $B(0, 0.99)$, $C(0.1, 0.9)$, and $D(0.9, 0.1)$.

In Figure 5, we plot the link between the entanglement and photon excitation's when the oscillators are resonant $\omega_1^2 = \omega_2^2 = 1.01$ ($\epsilon = 0$) for three values of coupling $J_0 = 0.1, 0.2, 0.3$. We observe that entanglement and vacuum excitation's are freezed during the half period $[0, \frac{\pi}{2}]$. This is due to the fact that dilatation functions (50-51) still constant in this interval. For $t > \frac{\pi}{2}$, the both quantities exhibit the same topological behavior ($\langle N \rangle \propto E_N$).

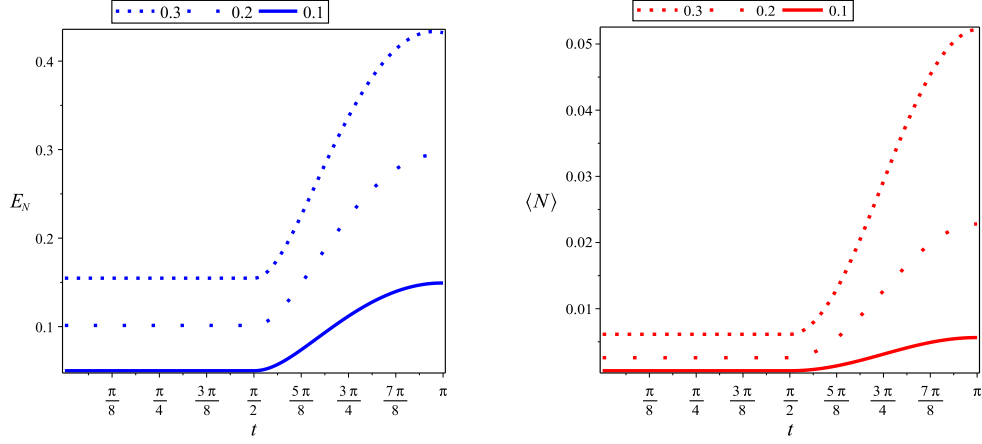


Figure 5 – (color online) Left panel presents the dynamics of entanglement quantified by Logarithmic negativity E_N and right panel shows the photon excitation's $\langle N_1 \rangle = \langle N_2 \rangle = \langle N \rangle$ for the parameters $\epsilon = 0$, $\omega_0^2 = 1.01$ and $J_0 = 0.1, 0.2, 0.3$.

In Figure 6, we investigate the effects of non-resonance on the geometric average of excitation's $M_{12}(t) = (\langle N_1(t) \rangle \langle N_2(t) \rangle)^{\frac{1}{2}}$ and entanglement. When $t \in [0, \frac{\pi}{2}]$ a tiny and constant amount of excitation's and entanglement are detected, but since $t > \frac{\pi}{2}$ the excitation's dramatically increase compared to the entanglement generation. We mention, although the excitation's are important the oscillators still weakly entangled and the maximum of entanglement is obtained when the excitation's are more hierarchical (i.e. $|\langle N_2(t) \rangle - \langle N_1(t) \rangle|$ reaches its maximal value). To conclude, the extinction of entanglement requires the condition $J_0 = 0$, but that of excitations requires resonance together with $J_0 = 0$. The photon excitation's generate important amounts of entanglement when oscillators are resonant ($\epsilon = 0$) and strongly coupled. This is similar to what has been found by considering time-independent coupled oscillators [6]. It turns out this phenomenon can be seen as the Casimir effect because the virtual photon exchange plays a vital role in mediating the coupling between oscillators [22]. Then they generate entanglement, but their contribution is perhaps limited by their quantum destructive interference, which becomes more important when the system moves away from the resonance ($\epsilon \rightarrow \omega_0^2$).

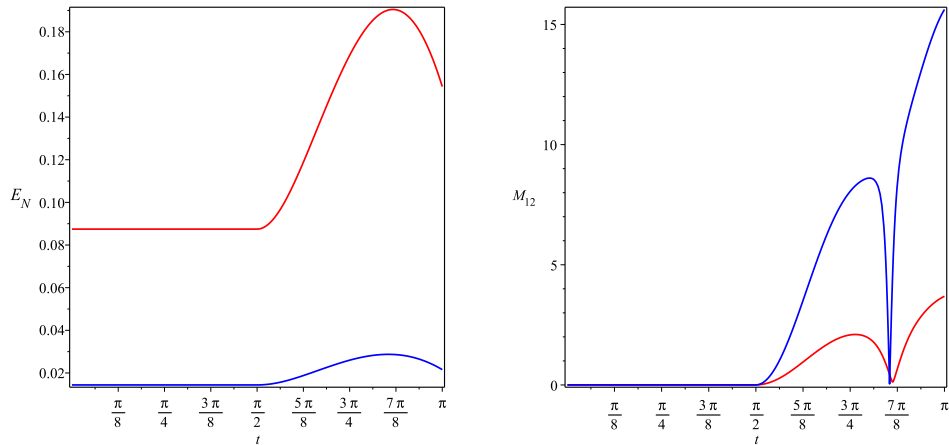


Figure 6 – (color online) Left panel presents the dynamics of entanglement quantified by logarithmic negativity $E_N(t)$. Right panel shows the geometric average of photon excitation's $M_{12}(t) = (\langle N_1 \rangle \langle N_2 \rangle)^{\frac{1}{2}}$. The configurations are taken $\omega_0^2 = 1.01$, (blue line) for $(\epsilon = 0.99, J_0 = 0.01)$ and (red line) for $(\epsilon = 0.9, J_0 = 0.1)$.

In Figure 7, we show the effects of coupling on entanglement $E_{\mathcal{N}}(t)$, geometric average of photon $M_{12}(t) = (\langle N_1(t) \rangle \langle N_2(t) \rangle)^{\frac{1}{2}}$, ($t \in [0, \pi/2]$), and we define $Ins := \Lambda(\Omega_1, \Omega_2) - 1$ as geometric quantifier of instability (32). We observe that the three quantities exhibit the same behavior with respect to coupling J_0 , they are monotonically increasing, which entails the importance of strong coupling physics [6]. It is worthy to note that $Ins(J_0 = 0, \epsilon = 0.1) \sim 0.005$ (oscillators are unstable), $E_{\mathcal{N}} = 0$ and $M_{12}(t) \neq 0$, similarly, $Ins(J_0 = 0, \epsilon = 0) \sim -1.2 \cdot 10^{-4}$ (oscillators are stable), $E_{\mathcal{N}} = 0$ and $M_{12}(t) = 0$. Finally, those similarities show that classical instabilities affect the generation of excitation's and hence entanglement between oscillators.

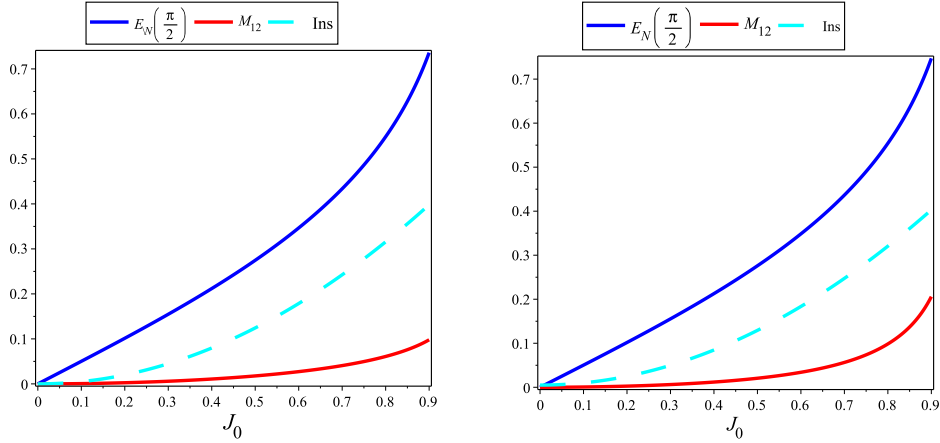


Figure 7 – (color online) Effects of coupling on entanglement $E_{\mathcal{N}}(\frac{\pi}{2})$, geometric average $M_{12} = (\langle N_1 \rangle \langle N_2 \rangle)^{\frac{1}{2}}$ and $Ins = \Lambda(\Omega_1, \Omega_2) - 1$, left panel: $\epsilon = 0$ and right panel: $\epsilon = 0.1$ with $\omega_0^2 = 1.01$.

6 Conclusion

We have studied two non resonant coupled harmonic oscillators connected by a periodically pumped coupling $J(t) = J_0 \times \Theta(t)$ and frequencies. We have solved exactly the Schrödinger dynamics, which leads to Ermakov differential equations. After a suitable transformations, we have showed that they are equivalent to classical counterparts of the decoupled quantum Hamiltonian. By studying the instability of the classical analog and computing the photon excitation's in the vacuum state, we have found that the excitation's will be created if the classical oscillators are unstable.

We have studied the dynamics of entanglement by computing logarithmic negativity together with photon excitation's beyond resonance by using phase space picture. We have analyzed the effects of coupling and quench amplitude on entanglement dynamics and photon excitation's. Consequently, it was found that photon excitation's present the same behavior when the oscillators are resonant and strongly coupled $J_0 \sim \omega_{1,2}^2$, and when the oscillators are non resonant and weakly coupled the photon's excitation's have a tiny contribution on entanglement generation. We have showed also that extinction of excitation's entails the suppression of entanglement. However, it does not imply necessarily the suppression of excitation's if the oscillators are separated. This allows us to conclude that the excitation's generate and maintain entanglement.

References

- [1] A. Einstein, B. Podolsky, and N. Rosen, Phys. Rev. 47, 777 (1935).
- [2] J. S. Bell, Physics 1, 195 (1964).
- [3] J. C. Gonzalez-Henao, E. Pugliese, S. Euzzor, S. F. Abdalah, R. Meucci and J. A. Roversi, Scientific Reports 5, 13152 (2015).
- [4] J. C. Gonzalez-Henao, E. Pugliese, S. Euzzor, R. Meucci, J. A. Roversi and F. T. Arecchi, Scientific Reports 7, 9957 (2017).
- [5] T. Figueiredo Roque and J. A. Roversi, Phys. Rev. A 88, 032114 (2013).
- [6] J.-Y. Zhou, Y.-H. Zhou, X.-L. Yin, J.-F. Huang and J.-Q. Liao, Scientific Reports 10, 12557 (2020).
- [7] E. Meissner, Schweizer Bauzeitung 72, 95 (1918).
- [8] J. A. Richards, *Analysis of periodically time-varying systems* (Springer-Verlag, Berlin, 1983).
- [9] A. A. Burov and V. I. Nikonov, Int. J. Non-Linear Mech. 110, 26 (2019).
- [10] E. Pinney, Proc. Am. Math. Soc. 1, 681, (1950).
- [11] D. X. Macedo and I. Guedes, J. Math. Phys. 53, 052101 (2012).
- [12] S. Menouar, M. Maamache and J. R. Choi, Physica Scripta 82, 6 (2010).
- [13] H. R. Lewis and W. B. Riesenfeld, J. Math. Phys. 10, 1458 (1969).
- [14] K. E. Thylwe and H. J. Korsch, J. Phys. A 31, L279–L285 (1998).
- [15] Xi Chen, A. Ruschhaupt, S. Schmidt, A. del Campo, D. Guéry-Odelin and J. G. Muga, Phys. Rev. Lett. 104, 063002 (2010).
- [16] A. Tobalina, E. Torrontegui, I. Lizuain, M. Palmero and J. G. Muga, Phys. Rev. A 102, 063112 (2020).
- [17] G. Adesso and F. Illuminati, Phys. Rev. A 72, 032334 (2005).
- [18] G. Adesso, A. Serafini and F. Illuminati, Phys. Rev. A 73, 032345 (2006).
- [19] Y. S. Kim and M. E. Noz, *Phase Space Picture of Quantum Mechanics* (World Scientific, Singapore, 1991).
- [20] M. A. Lohe, J. Phys. A: Math. Theor. 42, 035307 (2009).
- [21] K. H. Yeon, H. J. Kim, C. I. Um, T. F. George and L. N. Pandey, Phys. Rev. A 50, 1035 (1994).
- [22] D. L. Andrews and D. S. Bradshaw, Ann. Phys. 526, 173 (2014).